Applications of MpCCI-Based Fluid-Structure Interactions Coupling to Vibrational and Rotational Blades.

Yang Yang, William W. Liou (Western Michigan University, U.S.A.); Pascal Bayrasy (Fraunhofer-Institute for Algorithms and Scientific Computing SCAI, Germany)

1 Introduction

Fan blades have been widely used in many different areas, such as in jet engines, turbomachinery, wind turbines, cooling fans to moderate heating of internal combustion engines and etc. Failure of fan blades especially in heavy-duty machinery causes major financial losses to business and sometimes even fatal accidents. It is therefore the primary task for engineers to ensure a fan equipment to have a long and safe life for the designed operating condition. Loadings on the fan blades include both the centrifugal force and the fluctuating aerodynamic load, which are attributed to the frequent energy exchanges imparted by fluid-structure interactions between the fan blade body and the passing air flow. The fluid-structure interactions are important in the design of heavy-duty fan blades because the interactions lead to fatigue and ultimately structural damage of blades.

Modeling of the fluid-structure interactions in fan blades rotating at high speed is difficult as the blades undergo two types of deformation simultaneously. The first is the rotational motion of the blades which dictates overall position of the blades and the appropriate time step size for the corresponding computational schemes. The second is the local structural deformation of the blades due to the centrifugal and the aerodynamic forces, which is crucial in modeling the fluid-structure interactions. Successful implementation requires accurate solution mapping between the two non-conformal meshes and synchronization of mesh motions. To simplify the problem, most of older studies adopt the one-way coupling scheme meaning that only the aerodynamic loading is fed to the structural solver. some researchers used modal dynamics to solve the vibration of the fan blades by including the first and/or the second mode shape[1], [2]. Some used the blade element method to calculate the fluttering of the fan blades[3], which is based on 2D airfoil properties. Results from full 3D two-way coupling of solvers of the Reynolds-averaged Navier-Stokes (RANS) equations and the finite element analysis (FEA) for the linear elasticity are scarce. As reported in[4], coupling of the commercial software ANSYS CFX and ANSYS Structure were used to study the high-cycle fatigue of fan blades. A 3D rotor-stator mesh was constructed and calculated in the fluid domain however only one blade was modeled in the structure code.

In this study, the complete set of the RANS equations and the FEA equations are coupled via MpCCI[5] and solved for by commercial software packages ANSYS Fluent and Abaqus. The MpCCI establishes the bi-directional coupling interface between the two simulation codes. Solution data exchange is done automatically within MpCCI for the two non-matching mesh grids using the best-fit interpolation method. Additionally, for this particular fluid-structure interaction (FSI) problem with the rotating fan blades, the mesh motion needs to be taken into account with great care. In the following section, we will report results from the fully coupled FSI analysis for a generic fan rotating at a constant speed, where the complete 3D representation of the fan is retained without any simplification during the simulation.

2 Results and Discussion

In this section, we first present the results from an FSI analysis of a mixing element blade using MpCCI enabled coupling between Fluent and Abaqus. The obtained results are then compared with that from STAR-CCM+ enabled coupling where Abaqus is also used as the structural solver. The comparison serves as a form of verification of the FSI scheme used. In the second part, the fully coupled FSI analysis of a rotating fan using MpCCI enabled coupling scheme is presented.

2.1 FSI analysis of a mixing element blade

The geometry of the mixing element blade is shown in Figure 1 (a) and it is located in the center of the cylindrical domain as demonstrated in Figure 1 (b). A time varying pressure boundary condition is prescribed at the inlet boundary, which is representative of pressure fluctuation observed in practical applications. A constant pressure is prescribed at the outlet. The density of the air is $1.19\ \mathrm{kg}/m^3$ and the dynamic viscosity is $1.86{\times}10^{-5} PaS$.

To have an idea of how different the FSI analysis results will be between the MpCCI enabled scheme and the STAR-CCM+ enabled scheme, two models were built using the same geometry, mesh, initial conditions, time stepping scheme as well as the same FSI coupling scheme. The magnitude of the tip

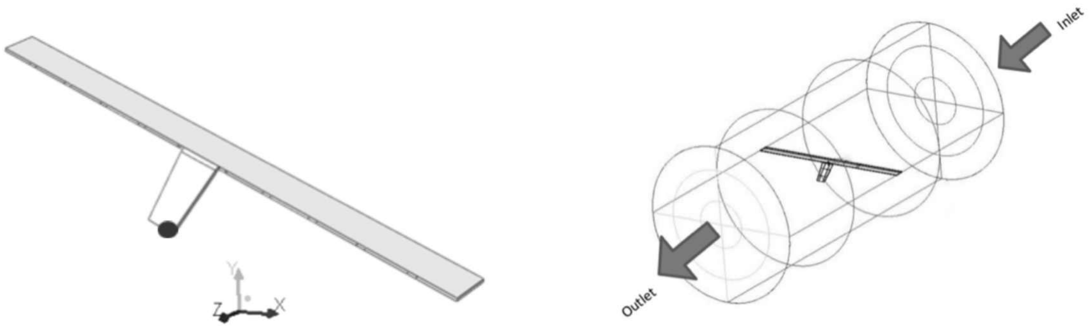

(a) (b)

Figure 1 Geometry and dimensions of the mixing element blade and the fluid domain.

displacement of the mixing element blade is recorded at the location denoted as the black dot shown in Figure 1 (a). Figure 2 (a) shows the comparison of the tip displacement. It can be seen that the prediction of the displacement agrees very well except that the MPCCI prediction overshoots by small amount. We find that the overshoot is due to fact that the pressure loading on the surface predicted by

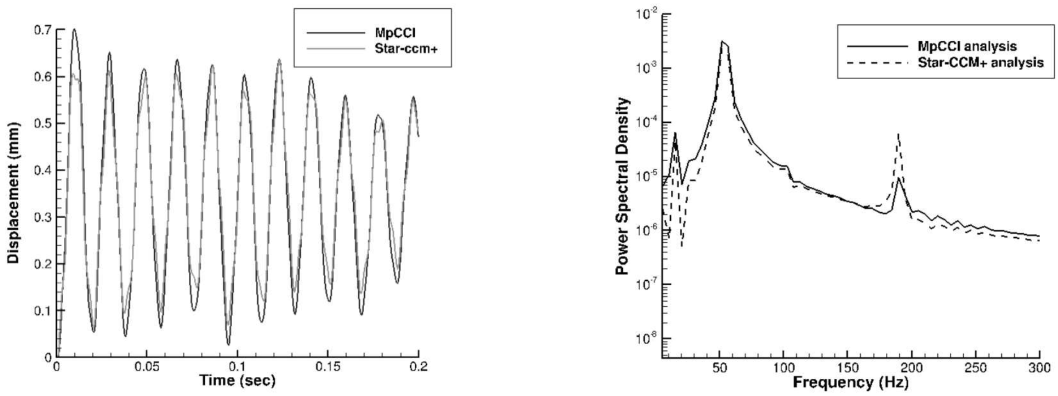

(a) (b)

Figure 2 Comparison of the tip displacement of the mixing element blade using MpCCI and STAR-CCM+.

Fluent is higher than that by STAR-CCM+. Signature frequencies are extracted using FFT and the comparison is presented in Figure 2 (b). It is clear that the dominant frequency predicted by the two methods is almost identically 52 Hz. The overall magnitude of the power spectral density matches well too. It is therefore verified that the results from the MpCCI enabled FSI analysis agree well with those from the STAR-CCM+ enabled analysis.

2.2 FSI analysis of a rotating fan

To simulate the FSI effects in a rotating fan, a unique FSI scheme was tested. As demonstrated in Figure 3, in Fluent, the sliding mesh method is applied to model the rotation of the fan and at the same time, the dynamic meshing is used to account for the local structural deformation of the blades caused

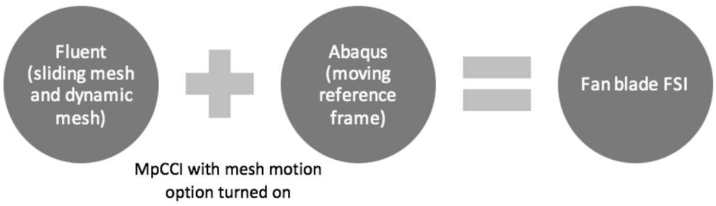

Figure 3 The unique FSI scheme.

by the centrifugal and aerodynamic loadings. In Abaqus, a moving reference frame is set up to take into account of the constant rotational speed. The two models are coupled by MpCCI. In the MpCCI model, the "mesh motion" option is turned on so that all incoming quantities and coordinates are transformed into a space-fixed reference system and all outgoing values are transformed back to the target reference frame. The fluid domain and the mesh of the rotating fan used in the Fluent model are shown in Figure 4 (a). 0.9 million tetrahedral elements are used in the mesh and the entire fluid domain is defined as the sliding mesh zone with a speed of 1700 rpm. Figure 4 (b) shows the Abaqus model and the direction of rotation of the fan. A moving reference frame with the same speed as in the fluid model is defined for the entire model. The hub region is constrained in space. 34K quadratic tetrahedral elements are used. As shown in Figure 5(a), the nodal distance that measures the closest geometric distance from each node of one mesh to a point of the other is plotted for both sides of the FSI meshes of the Abaqus and the Fluent model. Apparently the association of the two meshes is very tight. The mapping accuracy of quantities can be corroborated, as demonstrated in Figure 5(b), by comparing the pressure contours on the front and back side of the fan blades between the two models.

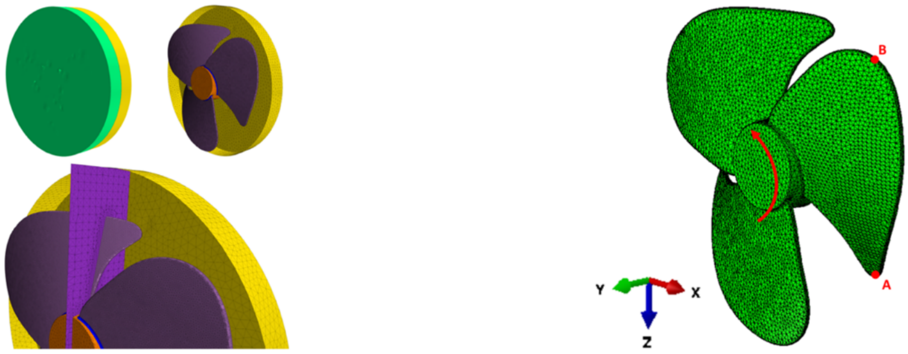

(a) (b)

Figure 4 Geometry and meshes of the rotating fan in Fluent and Abaqus models.

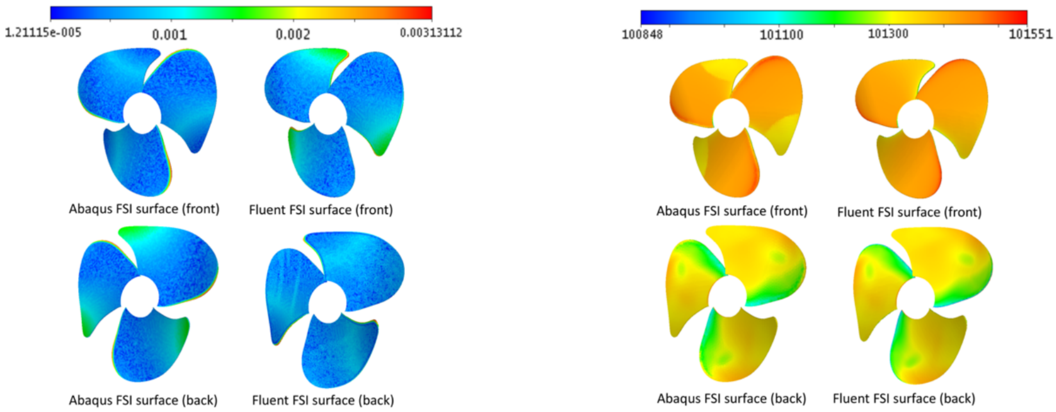

(a) Nodal distance (mm) of the FSI meshes (b) Overpressure (Pa) on the FSI meshes

Figure 5 Geometry comparison and mapping verification of the FSI meshes.

Influence of the FSI on the fan blades can be observed in Figure 6 where displacements of point A and B are presented for the case with the FSI effects (the FSI case) and the case without the FSI effects (the non-FSI case). For each case, three components of the displacement are plotted, Ux and Uz being the in-plane components while Uy being the axial component. By comparing the two cases, the oscillatory amplitudes of the displacement of both point A and B are larger in the FSI case than in the non-FSI case. For an example, in Uy, the averaged amplitude of point A for the FSI case is 30.8% higher than that for the non-FSI case; the same quantity of point B for the FSI case is 8.5 times for the non-FSI case.

Another demonstration of the effects of the FSI on the fan blades is the excited mode shapes. As shown in Figure 7, at 334 Hz, the fan tends to vibrate the most around point B on the three blades; while at 529 Hz, the highest vibration is near point A. FFT analyses of the displacement signals recorded during the non-FSI case, as plotted in Figure 6 (d) – (f), produce the same frequency of 505 Hz for either location, which indicates that when FSI effects not considered, only the second mode shape can be excited and the first mode or the deformation at point B is almost nonexistent. When the FSI effects are include, the FFT analysis of the displacement signals, as shown in Figure 6 (a) – (c), gives a lower frequency of 291 Hz and a higher frequency of 583 Hz corresponding to the two natural frequencies. In other words, the FSI excites the first mode shape or the more pronounced deformation and vibration at point B as already demonstrated in Figure 6 (a) – (c).

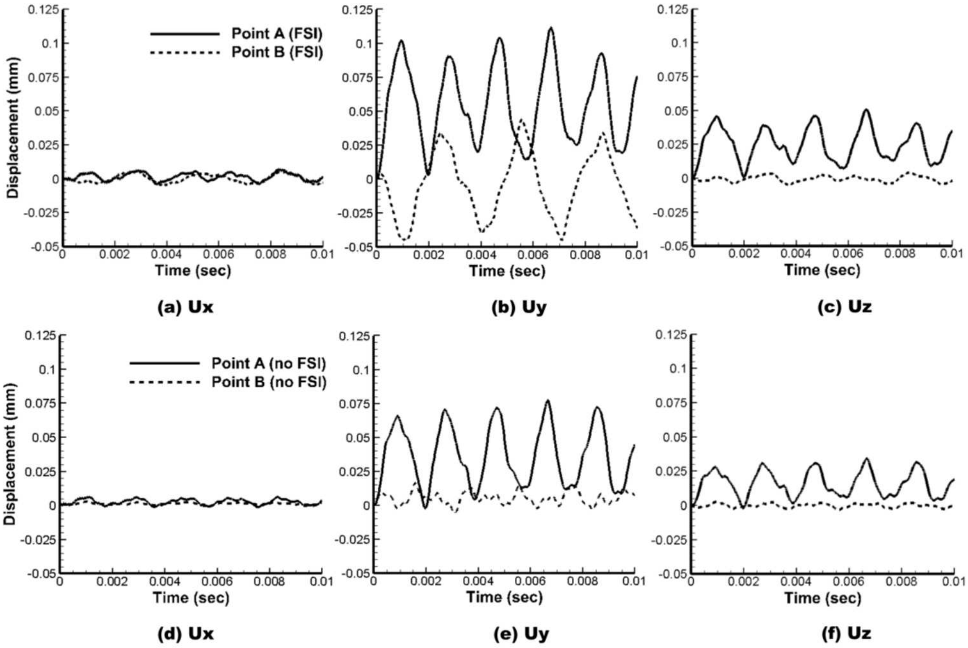

Figure 6 Displacement history of point A and B on the fan blade during the rotation with FSI and without FSI.

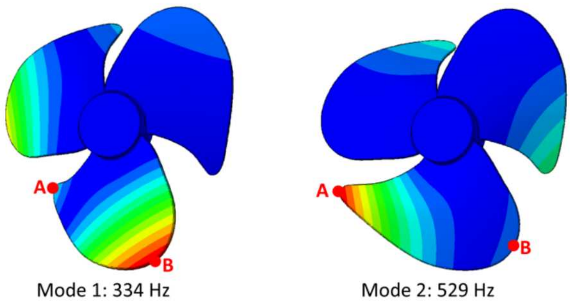

Figure 7 Two primary modes of the fan (natural frequency). Contours by displacement magnitude. The red and the blue color represents the maximum and the minimum displacement respectively.

3 Conclusions

In this study, we used the MpCCI tool to couple ANSYS Fluent and Abaqus in an effort to solve an FSI problem of vibrational and rotational fan blades. Sliding mesh method was used in the Fluent model and the moving reference frame used in the Abaqus model. Coordinate transformation due to the mesh motion was handled by the MpCCI tool. We verified the MpCCI tool by comparing the results from a vibrating mixing element blade with those from a STAR-CCM+ moderated FSI model. The difference of the two results were insignificant. For the rotating fan FSI problem, we successfully implemented the scheme and the results show the influence of the FSI on the overall response of the fan blades, which is important to prevent fan blades rotating at high speed from failure due to fatigue.

4 References

[1] Y. Zheng and H. Yang, "Coupled fluid-structure flutter analysis of a transonic fan," *Chinese J. Aeronaut.*, vol. 24, no. 3, pp. 258–264, 2011.

[2] D. G. Holmes and H. A. Chuang, "2D Linearized Harmonic Euler Flow Analysis for Flutter and Forced Response," in *Unsteady Aerodynamics, Aeroacoustics, and Aeroelasticity of Turbomachines and Propellers*, New York, NY: Springer New York, 1993, pp. 213–230.

[3] F. Rasmussen, M. H. Hansen, K. Thomsen, T. J. Larsen, F. Bertagnolio, J. Johansen, H. A. Madsen, C. Bak, and A. M. Hansen, "Present Status of Aeroelasticity of Wind Turbines," *Wind Energy*, vol. 6, no. 3, pp. 213–228, Jul. 2003.

[4] P. Dhopade, A. J. Neely, J. Young, and K. Shankar, "High-Cycle Fatigue of Fan Blades Accounting for Fluid-Structure Interaction," in *Proceedings of ASME Turbo Expo*, 2012, p. 1365.

[5] *MpCCI 4.4.0 documentations*. Fraunhofer SCAI, 2015.